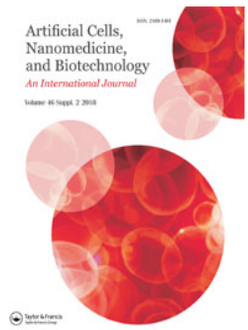

Taylor & Francis
Taylor & Francis Group

Artificial Cells, Nanomedicine, and Biotechnology

An International Journal

ISSN: 2169-1401 (Print) 2169-141X (Online) Journal homepage: https://www.tandfonline.com/loi/ianb20

Melatonin-stimulated biosynthesis of anti-microbial ZnONPs by enhancing bio-reductive prospective in callus cultures of *Catharanthus roseus* var. *Alba*

Hafiza Rida Riaz, Syed Salman Hashmi, Tariq Khan, Christophe Hano, Nathalie Giglioli-Guivarc'h & Bilal Haider Abbasi

To cite this article: Hafiza Rida Riaz, Syed Salman Hashmi, Tariq Khan, Christophe Hano, Nathalie Giglioli-Guivarc'h & Bilal Haider Abbasi (2018) Melatonin-stimulated biosynthesis of anti-microbial ZnONPs by enhancing bio-reductive prospective in callus cultures of *Catharanthus roseus* var. *Alba*, Artificial Cells, Nanomedicine, and Biotechnology, 46:sup2, 936-950, DOI: 10.1080/21691401.2018.1473413

To link to this article: https://doi.org/10.1080/21691401.2018.1473413

Published online: 18 May 2018.

ARTIFICIAL CELLS, NANOMEDICINE, AND BIOTECHNOLOGY
2018, VOL. 46, NO. S2, S936–S950
https://doi.org/10.1080/21691401.2018.1473413

Melatonin-stimulated biosynthesis of anti-microbial ZnONPs by enhancing bio-reductive prospective in callus cultures of *Catharanthus roseus* var. *Alba*

Hafiza Rida Riaz[a], Syed Salman Hashmi[a], Tariq Khan[a,b], Christophe Hano[c], Nathalie Giglioli-Guivarc'h[d] and Bilal Haider Abbasi[a,c,d]

[a]Department of Biotechnology, Quaid-i-Azam University, Islamabad, Pakistan; [b]Department of Biotechnology, University of Malakand, Chakdara Dir Lower, Pakistan; [c]Laboratoire de Biologie des Ligneux et des Grandes Cultures (LBLGC), UPRES EA 1207, Université d'Orléans, Chartres, France; [d]EA2106 Biomolécules et Biotechnologies Végétales, Université de Tours, Tours, France

ABSTRACT

Melatonin as plant growth regulator induces differential effects on metabolites that are responsible for reduction, capping and stabilization of zinc oxide nanoparticles. Phytochemical analysis of callus cultures was performed and results were compared with callus cultures supplemented with other plant growth regulators (α-napthalene acetic acid, 2,4-dichlorophenoxy acetic acid and thidiazuron). Highest total phenolic and flavonoid content [42.23 mg of gallic acid equivalent (GAE) g^{-1} DW and 36.4 mg of (quercetin equivalent) g^{-1} DW, respectively] were recorded at melatonin (1.0 μM) + NAA (13.5 μM). ZnONPs were synthesized from NAA (13.5 μM) and melatonin (1.0 μM) + NAA (13.5 μM)-induced calli extracts separately and characterized via X-ray diffraction, Fourier transform infrared spectroscopy (FTIR) and scanning electron microscopy (SEM). FTIR analysis confirmed the presence of phenolics and flavonoids that were mainly found responsible for reduction and capping of ZnONPs. SEM analysis showed triangular shaped ZnONPs synthesized from melatonin + NAA callus extract and these NPs were more dispersed as compared to the spherical-agglomerates of ZnONPs synthesized from NAA-mediated callus extract. Melatonin + NAA callus extract-mediated ZnONPs (having smaller size) were more potent against multiple drug resistant bacterial strains, e.g. *Bacillus subtilis, Escherichia coli* and *Pseudomonas aeruginosa* by producing zone of inhibitions 17 ± 0.76 mm,10 ± 0.57 mm and 13 ± 0.54 mm, respectively.

ARTICLE HISTORY

KEYWORDS

Catharanthus; bio-reduction; phytochemicals; ZnONPs; biomedical

Introduction

Zinc oxide (ZnO) nanoparticles (NPs) belong to the class of metal oxide NPs, which are non-toxic, less expensive and readily available, having high catalytic, UV blocking, light trapping, anti-fungal and anti-microbial activities. It is considered best and safe material in many organic transformations to act as a catalyst [1–5]. Also, there are a number of biomedical applications of ZnONPs including anti-bacterial properties, which are much higher even at low concentrations with a possible reason being the disruption of bacterial lipid bilayers [6]. ZnONPs exhibit strong inhibitory activities against different multiple drug-resistant strains, e.g. *Bacillus subtilis, Escherichia coli, Klebsiella pneumonia, Salmonella typhi* and *Pseudomonas aeruginosa* [7]. ZnONPs have been synthesized by using biological, physical and chemical methods. Chemical methods include sonochemical, solvothermal, sol-gel and gel precipitation. Chemicals used for reduction and stabilization of NPs are mainly toxic and produces by-products that are not environment-friendly and sometimes it gets attached to the NPs surface thus producing severe effect during its applications [8]. Biological methods use microorganisms, plants, yeasts and fungi as a bioreactor for NPs synthesis [9,10]. Micro-organisms involve an elaborate process of maintaining cell cultures, multiple purification steps and intracellular synthesis [2]. Recently, phyto-nanotechnology gained much importance within few years as the process is simple, inexpensive, less time consuming, produces stable NPs and yields non-toxic by-products [9,11].

Catharanthus (*C.*) *roseus* (L.) G. Don var. *alba* is a medicinally important plant associated with Apocynaceae family. *Catharanthus roseus* was commonly known as Periwinkle or Madagascar-periwinkle found in various tropical and sub-tropical regions [12]. *Catharanthus roseus* having two varieties, white-flowered "alba" and pink-flowered "rosea" [13,14]. *Catharanthus roseus* is an alkaloid rich plant having >400 alkaloids from which >130 are TIAs (terpenoid-indole alkaloids) [15]. Vinca alkaloids such as vincristine and vinblastine are very popular for their use in cancer treatments [14,16]. Reserpine, serpentine and ajmalicine acts as anti-neuro-inflammatory and anti-hypertensive agents [15,17]. Vindoline, vindolidine and vindolicine are important for anti-diabetic activity [18]. ZnONPs have been synthesized using *C. roseus* leaves [19]. However, the potential of *C. roseus* callus cultures for ZnONPs synthesis has not been investigated till date. *Catharanthus roseus* is a rich source of bioactive agents other than alkaloids, e.g. phenolics, carbohydrates, flavonoids and saponins that help in reduction and stabilization process

CONTACT Bilal Haider Abbasi bhabbasi@qau.edu.pk Department of Biotechnology, Quaid-i-Azam University, Islamabad, Pakistan

during NPs synthesis [19,20]. Plant growth regulators (PGRs) are responsible for improved content of these bioactive agents in *in-vitro* cultures [21–23].

Melatonin (*N*-acetyl-5-tryptamine) is a PGR and belongs to the family indole-amines [24,25]. It governs the growth of explants, shoots and roots. It helps in activation of rhizogenesis and delays leaf senescence [26]. Melatonin, having the natural antioxidant capacity, plays an important role during abiotic stress such as heat, salinity, cold, drought, UV-radiation, herbicides and chemical pollutants [27,28]. Melatonin proved to be efficient in inducing defence either local or systematic against photo-oxidative stress [29]. It plays important role in photoperiodism such as flowering [30]. Melatonin has been reported for enhanced Ag-NPs synthesis by improving bio-reductive potential [19]. In the present work, melatonin is investigated for enhanced ZnONPs synthesis and anti-bacterial efficacy by improving phytochemical constituents when applied exogenously in callus cultures of *C. roseus*. Further, melatonin is compared with other PGRs (NAA, Kin, TDZ and 2,4-D) for its potential to improve the phytochemical status of *C. roseus* callus cultures.

Material and methods

Plant collection

Catharanthus roseus var. *Alba* mature and fresh green leaves were collected from the Department of Biotechnology, Quaid-i-Azam University Islamabad. Washing was done with distilled-water to stave off all the debris and taken to the laminar flow. Further, leaves were treated for 15 s with 1% mercuric chloride solution and washed five times with autoclaved distilled water. After that, leaves were placed onto autoclaved filter paper discs for drying.

Establishment of callus cultures from the wild plant

Leaf explants of 1–2 cm were inoculated on MS (Murishage and Skoog, 1962) medium containing 30 g of sucrose and 8 g of agar. PGRs NAA, Kin, TDZ and 2,4-D were added into media in various concentrations, e.g. 2.25 μM, 4.5 μM, 9.0 μM and 13.5 μM. Before autoclaving, pH was adjusted between 5.6 and 5.7 by using 1 N NaOH and 1 N HCl according to the procedure of Abbasi et al. [31]. All the work was done under laminar flow. Three explants were inoculated in each conical flask as one replicate for one PGR concentration and experiment was performed with three replicates. Flasks were transferred to the growth room and kept under 16/8-h photoperiod at temperature of 25 °C ± 2 °C. After 28 d of inoculation, Calli fresh weight (FW) and dry weight (DW) was recorded and callus induction frequencies (CIF) was calculated by following formula:

$$\text{Callus induction frequency}\,(\%) = \frac{\text{No. of the explants producing callus}}{\text{Total no. of the explants in the culture}} \times 100$$

CIF represents the percentage of explants which induced callus. Callus produced on NAA 13.5 μM (having highest phytochemical contents) was selected as control callus and sub-cultured with various concentrations of melatonin (0.5, 1, 2, 3, 4, 5, 10, 15 and 20 μM) + 13.5 μM NAA.

Phytochemical analysis

Extract preparation

Calli produced on different PGRs concentrations were collected, dried and ground into fine powder. A total of 200 mg of powders were separately mixed into 1500 μL of methanol for extract preparation and left on rotator shaker for 24 h. Mixtures were sonicated for 5 min and vortexed for proper mixing and shaking. This procedure was repeated three times and extracts were centrifuged at 13,000 rpm for 15 min. Supernatants were collected and stored at 4 °C for further use.

Total phenolic production

Total phenolic content (TPC) was determined by using the procedure of Singleton and Rossi [32] with slight amendments. Folin-Ciocalteu's reagent was used and dissolved in deionized H_2O. About 6 g of sodium carbonate was dissolved in 100 ml H_2O to prepare 6% solution and 4 mg of gallic acid dissolved in methanol. Absorbance was taken at 630 nm by using microplate reader. Gallic acid was used as standard and calibration curve was plotted (5 μg mL^{-1}, 10 μg mL^{-1}, 15 μg mL^{-1}, 20 μg mL^{-1} and 25 μg mL^{-1}, R_2= 0.967). TPC was expressed as mg of GAE g^{-1} DW and total phenolic production (TPP) was calculated by using the formula:

$$\text{TPP}\ (\text{mgL}^{-1}) = \text{TPC}\ (\text{mg of GAE g}^{-1}\,\text{DW}) \times \text{DW}\ (\text{g L}^{-1})$$

Total flavonoid production

Total flavonoid content (TFC) was determined by using the procedure of Ul-Haq et al. [33]. About 10% aluminium chloride and 1 M potassium acetate were dissolved in H_2O separately and 4 mg mL^{-1} quercetin dissolved in methanol for preparation of stock solutions. Absorbance was taken at 415 nm by using microplate reader. Quercetin was used as a standard and calibration curve was plotted (2.5 μg mL^{-1}, 5 μg mL^{-1}, 10 μg mL^{-1}, 2 μg mL^{-1} and 40 μg mL^{-1}, R_2 = 0.997). TPC was expressed as mg of QUE g^{-1} DW and total flavonoid production (TFP) of various PGRs concentrations was measured by using following formula:

$$\text{TFP}\ (\text{mgL}^{-1}) = \text{TFC}\ (\text{mg of QE g}^{-1}\,\text{DW}) \times \text{DW}\ (\text{g L}^{-1})$$

DPPH: FRSA (free radical scavenging activity)

Free radical scavenging activity (FRSA) of calli was determined by using DPPH (2,2-diphenyl-picrylhydrazyl) free radical. FRSA was carried out by following the procedure described by Rattanachitthawat et al. [34] with slight modifications. About 3.2 mg of DPPH was dissolved in 100 ml methanol as a stock solution and 4 mg mL^{-1} ascorbic acid in methanol and kept at room temperature for 30 min. Absorbance was taken at 517 nm. FRSA was calculated by

using following formula:

$$\% \text{ scavenging DPPH free radical} = 100 \times (1 - AE/AD)$$

where, the AE is the absorbance of the samples and AD is the absorbance of the DPPH solution.

Calli extract preparation for ZnONPs biosynthesis

Extracts for ZnONPs synthesis were prepared by adding 15 g of control callus (13.5 μM of NAA; Figure 1) and callus produced at melatonin (1 μM) + NAA (13.5 μM) separately dissolved in 100 ml distilled H_2O in Erlenmeyer flask (500 ml) and boiled for 8 min (Figure 1). NAA callus extract (NAA CE) and melatonin + NAA callus extract (Mel + NAA CE) were cooled down to room temperature and filtration was carried out with Whatman no. 1 filter paper. The volume of filtrates was adjusted to 100 ml and stored at 4 °C for further use.

Synthesis of ZnO NPs

A total of 5 ml of NAA CE and Mel + NAA CE was separately dissolved in 50 ml of 0.02 M Zinc acetate dihydrate solution (ZADS). After mixing, 2 M NaOH was added dropwise until the pH reached to 12. Pale-white (in the solution having NAA CE) and dark yellowish-pale precipitates (in the solution having Mel + NAA CE) appeared after completion of the reaction. Solution was left for 2 h under constant stirring. Centrifugation was carried out at 10,000 rpm for 10 min and washed two times with distilled H_2O to remove any impurities and left in the incubator overnight at 60 °C for complete transformation of $Zn(OH)_2$ into ZnO-NPs.

Characterization of ZnO nanoparticles

X-ray diffraction (XRD)

Crystalline nature of NAA CE and Mel + NAA CE-mediated ZnO NPs were confirmed through XRD by using the Shimadzu-Model XRD 6000 and the range of 2θ angles was 20°–80°. NPs sizes were calculated by using Debye-Scherrer equation $D = k\lambda/\beta\theta\cos$ (θ = Bragg's angle, λ = X-Ray wavelength (1.5421 Å), β = Full width at half maximum in radians and k = Shape factor (0.94).

Fourier transform infrared spectroscopy (FTIR)

FTIR was used to analyze various functional groups attached on the surfaces of NPs that are responsible for reduction, capping and stabilization of ZnO NPs. Perkin Elmer model having a mode of transmittance ranges between 4000 and 500 cm^{-1} was used. KBr pellets were used to record the sample on FTIR spectroscopy at room temperature.

Scanning electron microscopy (SEM)

Morphology of synthesized ZnO NPs from NAA CE and Mel + NAA CE were confirmed by SEM analysis by using SIGMA (MIRA3 TESCAN model) operated at 10 kV. Sample was dropped on the carbon-coated copper grid. Very thin film of samples were left to be dried for 5 min under mercuric lamp and images were taken under various magnifications.

Anti-bacterial assay

ZnO NPs efficacy was checked against multiple drug-resistant Gram-positive strain, e.g. *B. subtilis* (ATCC-21332) and

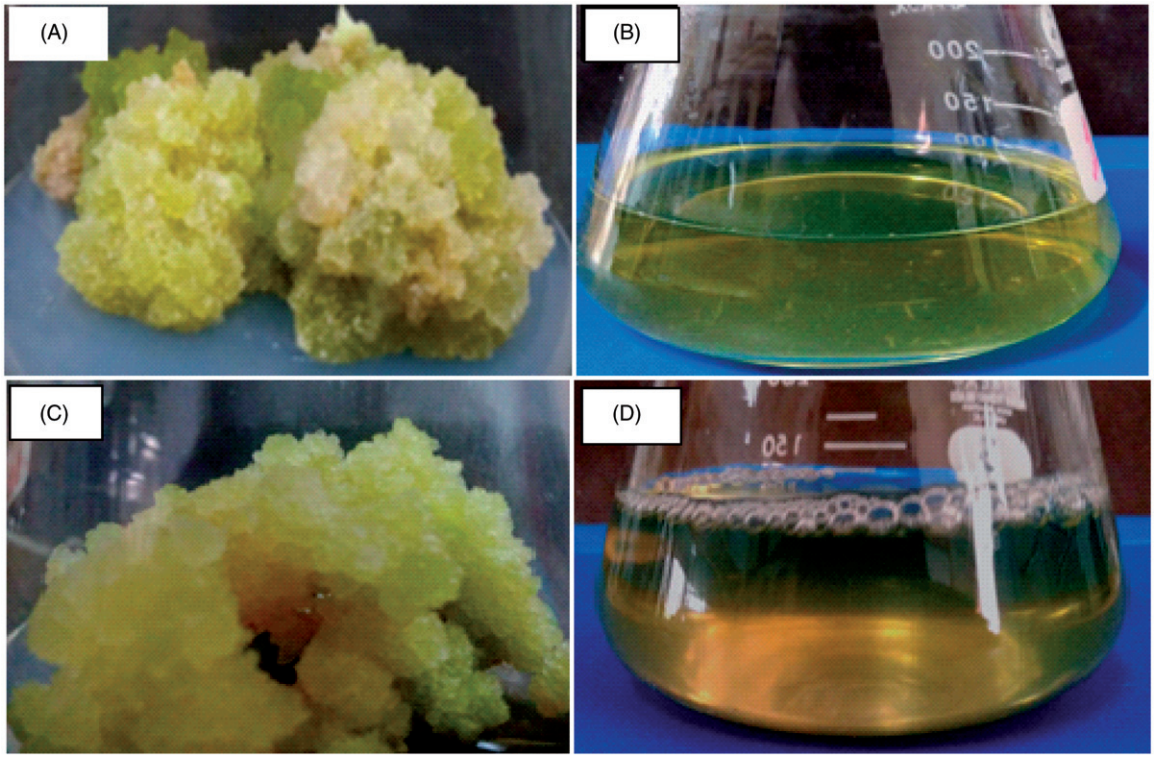

Figure 1. Extract preparation (A) control callus (13.5 μM of NAA) (B) NAA callus extract (NAA CE) (C) Mel (1 μM) + NAA (13.5 μM) induced callus (D) Mel + NAA callus extract (Mel + NAA CE).

Gram-negative strains *E. coli* (ATCC-15244) and *P. aeruginosa* (ATCC-27853) by using the procedure of Azam et al. [35] with slight amendments. ZADS was used as positive control. NAA CE and Mel + NAA CE callus extracts were used as negative control. Antibiotic amoxicillin was used as a standard. Bacterial strains were sub-cultured in nutrient broth (1.5 g of TSB dissolved in 100 ml distilled water) overnight for inoculum preparation. Anti-bacterial efficacy of ZnO NPs was assessed by using the well diffusion method. A solution of ZnO NPs was prepared by adding 1 mg of ZnO NPs in 1 ml distilled water. Bacterial cultures were swabbed separately on the nutrient agar plates with the help of cotton swabs and wells were created in the plates. About 20 μL solution of NAA CE and Mel + NAA CE-mediated ZnO NPs, ampicillin (10 mg mL^{-1} solution (standard), 0.02 M ZADS (positive control), whole plant extract (WPE), NAA CE and Mel + NAA CE was poured into the wells and incubated for 24 h at 30 °C. Data were collected from the experiments that were repeated thrice and zone of inhibition (mm) was calculated.

Results and discussion

Callus induction frequency % (CIF)

Callogenesis occurred on media supplemented with NAA, 2,4-D, kinetin and TDZ (2.25 μM, 4.5 μM, 9 μM and 13.5 μM). NAA, 2,4-D and NAA showed the best responses over callogenesis (Figure 2), while even a single concentration of kinetin did not show any response for callus induction.

CIF was 100% at NAA (4.5 and 13.5 μM) and 2,4-D (2.25 and 9 μM). CIF was 88% at 4.5 μM of 2,4-D (Figure 3). These results were similar to the findings of Upadhyaya et al. where NAA and 2,4-D were recorded best for callogenesis in *C. roseus* var. *nirmal* [36]. However, 13.5 μM NAA reported best for callus induction [37]. About 2 mg L^{-1} (9 μM) of 2,4-D is widely exploited for callogenesis and proved best for callus induction by various studies [13,36–39]. Auxin type and concentration always played an important role besides genotype because fluctuation in exogenous auxin concentration affect the callus initiation and proliferation efficiency [38].

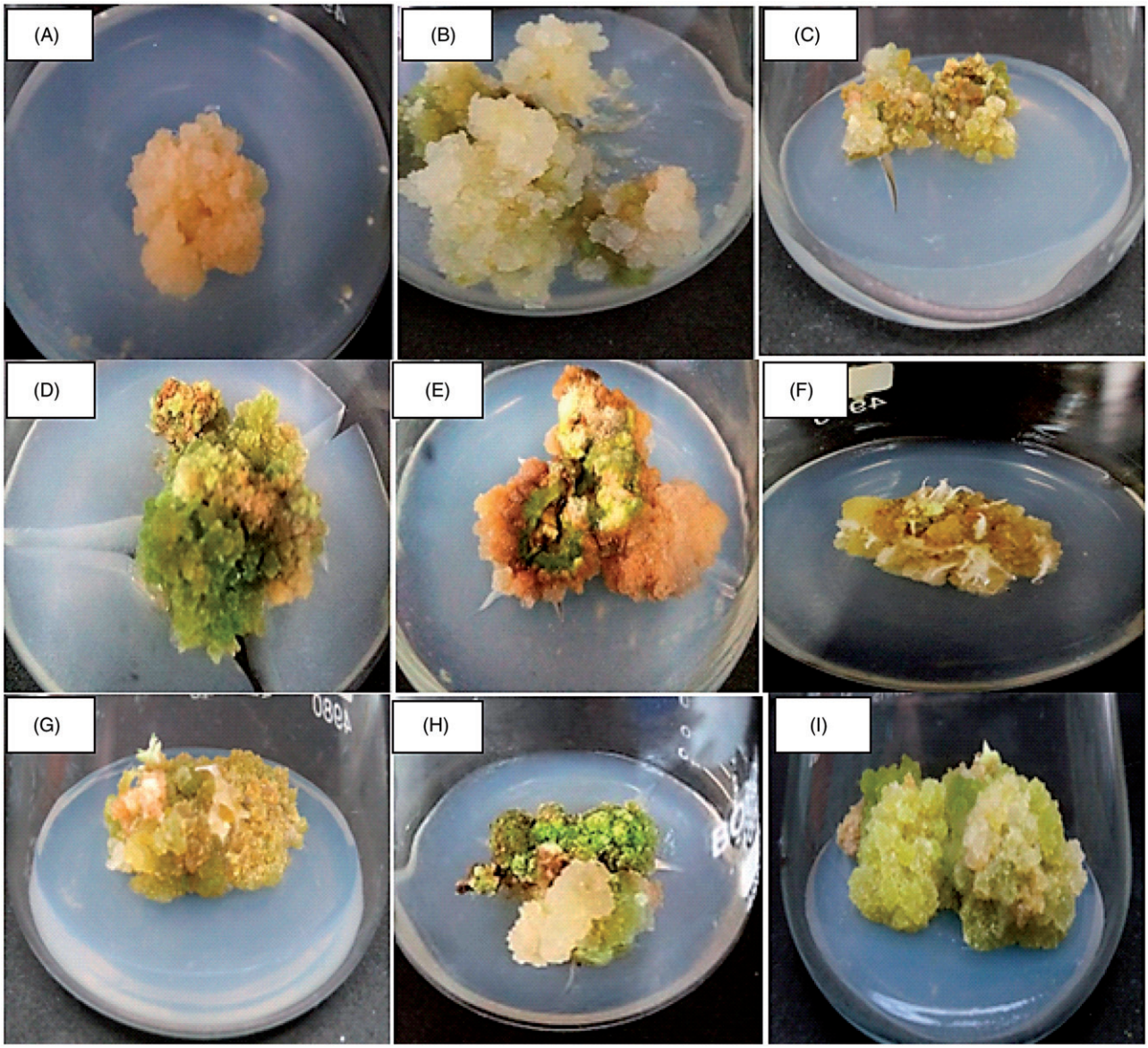

Figure 2. Calli formation on different PGRs concentrations (A) 2.25 μM 2,4-D (B) 9 μM 2,4-D (C) 13.5 μM 2,4-D (D) 2.25 μM TDZ (E) 4.5 μM TDZ (F) 9 μM TDZ (G) 2.25 μM NAA (H) 2.25 μM NAA (I) 13.5 μM NAA.

Highest CIF of 2,4-D might be due to its role in DNA synthesis and mitosis [40]. Lowest CIF (33.3 and 22.2%) was recorded at 2.25 and 13.5 μM of TDZ, respectively, and these results are relevant with the findings of Gill and Ozias-akins [41,42]. In the presence of higher levels of cytokinin, endogenous auxin concentration becomes lower and causes growth inhibition [43].

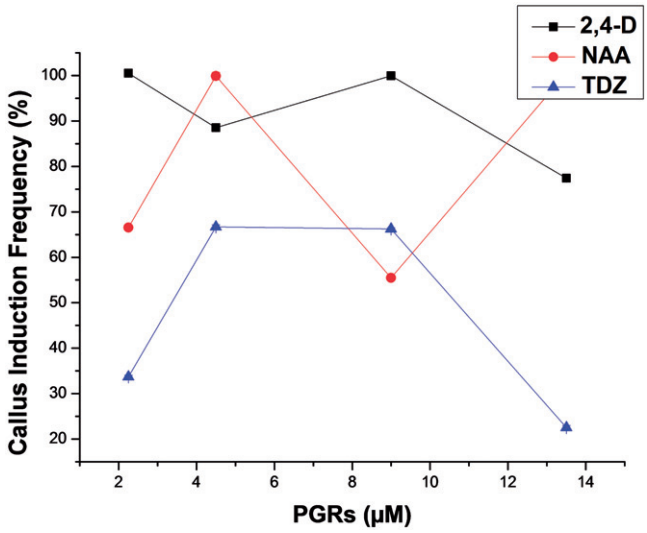

Figure 3. Callus induction frequency % (CIF) for different concentrations of NAA, 2,4-D and TDZ.

Sub-culturing with melatonin

Callus induced on 13.5 μM NAA was selected as control (having highest phytochemical contents) and sub-cultured on media supplemented with various concentrations of melatonin (0.5, 1, 2, 3, 4, 5, 10, 15 and 20 μM) + 13.5 μM NAA. Callus induction occurred on all the exogenously applied concentrations of melatonin (Figure 4). Melatonin is an auxin like-PGR [27], when applied exogenously helps in the formation of mitotic spindles and disrupts mitosis in many plants hence playing vital role in organogenesis and callogenesis in *in-vitro* derived cultures [30,44].

Table 1. Calli fresh weight (FW) and dry weight (DW) for different concentrations (μM) of NAA (α-naphthalene acetic acid, 2,4-D (2,4-dichlorophenoxy acetic acid and TDZ (thidiazuron), color of calli (dark brown (DB), brown (B), milky (M), light green (LG), texture of calli (friable (F) and compact (C).

		Callogenesis			
Hormones	Conc. (μM)	FW (g L^{-1})	DW (g L^{-1})	Color	Texture
NAA	2.25	65.5	4.25	LG	F
	4.5	83.10	6.91	LG	F
	9	113.08	8.5	LG	F
	13.5	121.45	8.86	LG	F
TDZ	2.25	35.75	3.7	DG + B	F
	4.5	70.75	6.71	DG + B	C
	9	75.56	6.74	DG + B	C
	13.5	55.2	4	DG + B	C
2,4-D	2.25	97.75	7.01	M	F
	4.5	101.7	7.25	M + LG	F
	9	90	6.67	M + LG	F
	13.5	119.37	7.78	LG	F

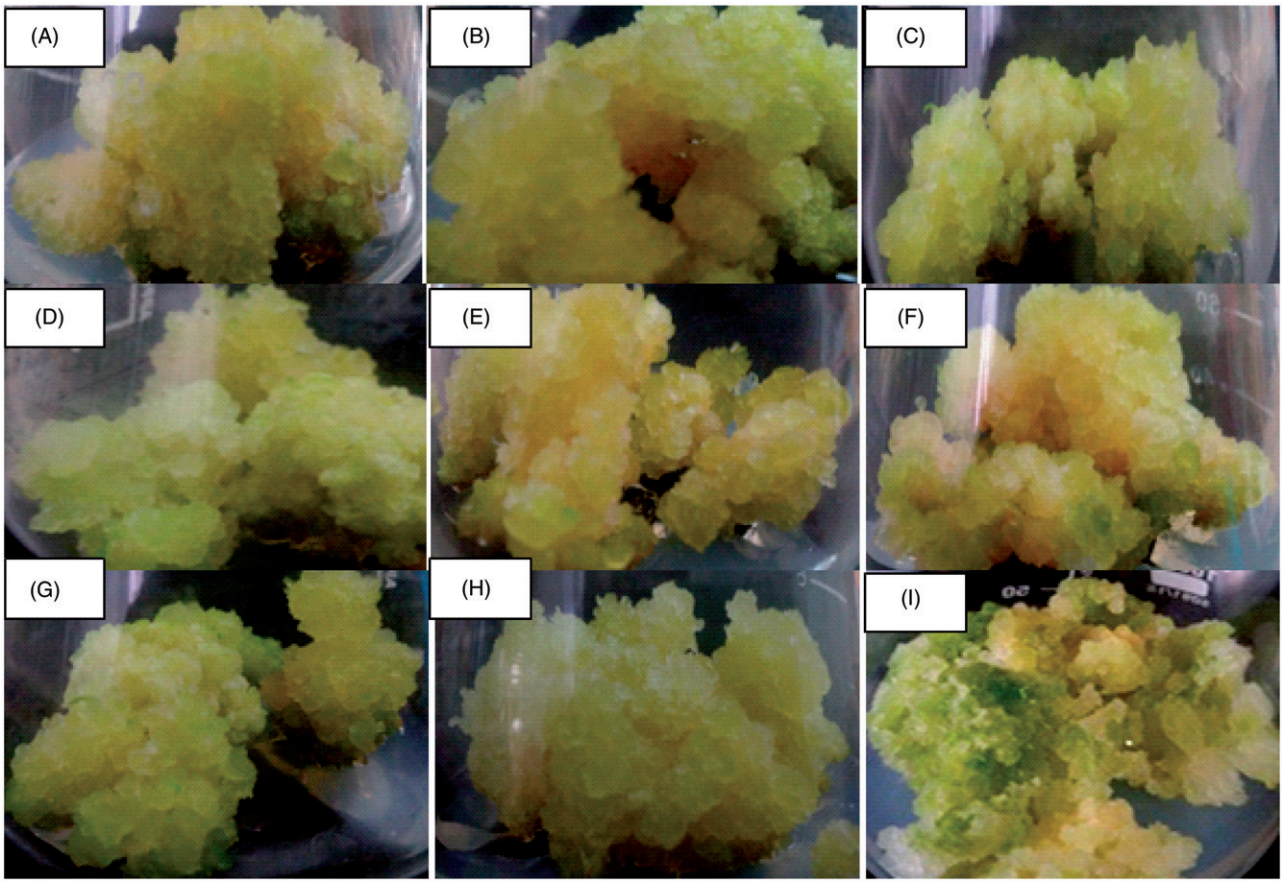

Figure 4. Callogenesis at different concentrations of melatonin (μM) + 13.5 NAA (A) 0.5 (B) 1 (C) 2 (D) 3 (E) 4 (F) 5 (G) 10 (H) 15 (I) 20.

Estimation of biomass accumulation

Biomass accumulation was maximum at NAA 4.5 μM and 13.5 μM (FW = 113.08 g L^{-1}, DW = 8.5 g L^{-1} and FW = 121.45 g L^{-1}, 8.86 g L^{-1}, respectively). Biomass accumulation (FW = 101.7 g L^{-1} and DW = 7.25 g L^{-1}) was recorded at 2,4-D (9 μM) (Table 1). NAA and 2,4-D reported best for callus induction and biomass accumulation [36,37]. Lowest values of FW (35.7 g L^{-1}) and DW (3.1 g $L^{-1)}$ was recorded at 2.25 μM of TDZ. Calli produced in response to the 2,4-D's various concentrations were milky to light green in color and texture of calli were friable. Dark green to brown colored callus was produced in response to TDZ. Calli produced on NAA's different concentrations was light green in color. Callus at 13.5 μM NAA was further sub-cultured with melatonin various concentrations (0.5, 1, 2, 3, 4, 5, 10, 15 and 20 μM) + 13.5 μM NAA. About 1 μM melatonin concentration showed highest biomass accumulation of FW (167.75 g $L^{-1)}$ and DW (9.825 g L^{-1}**)** and lowest values of FW (89.67 g $L^{-1)}$ and DW (5.2 g $L^{-1)}$ were recorded at melatonin (15 μM) (Table 2). The texture of calli was friable and light green in color.

Table 2. Calli fresh weight (FW) and dry weight (DW) for different concentrations (μM) of melatonin +13.5 μM NAA (α-naphthalene acetic acid), color of calli (yellow-green; YG) and texture of calli (friable; F).

	Callogenesis			
Melatonin (μM) + NAA (μM)	FW (g L^{-1})	DW (g L^{-1})	Color	Texture
0.5 + 13.5	145.23	9.2	YG	F
1 + 13.5	167.75	9.825	YG	F
2 + 13.5	112.45	7.5	YG	F
3 + 13.5	123.64	8.4	YG	F
4 + 13.5	89.11	6.02	YG	F
5 + 13.5	154.37	9.3	YG	F
10 + 13.5	127.67	8.56	YG	F
15 + 13.5	97.01	7.3	YG	F
20 + 13.5	101.0	7.42	YG	F

Estimation of total phenolic content (TPC) and production (TPP)

Phenolic profile of a plant represents its potential to overcome oxidative stress by scavenging free radical species

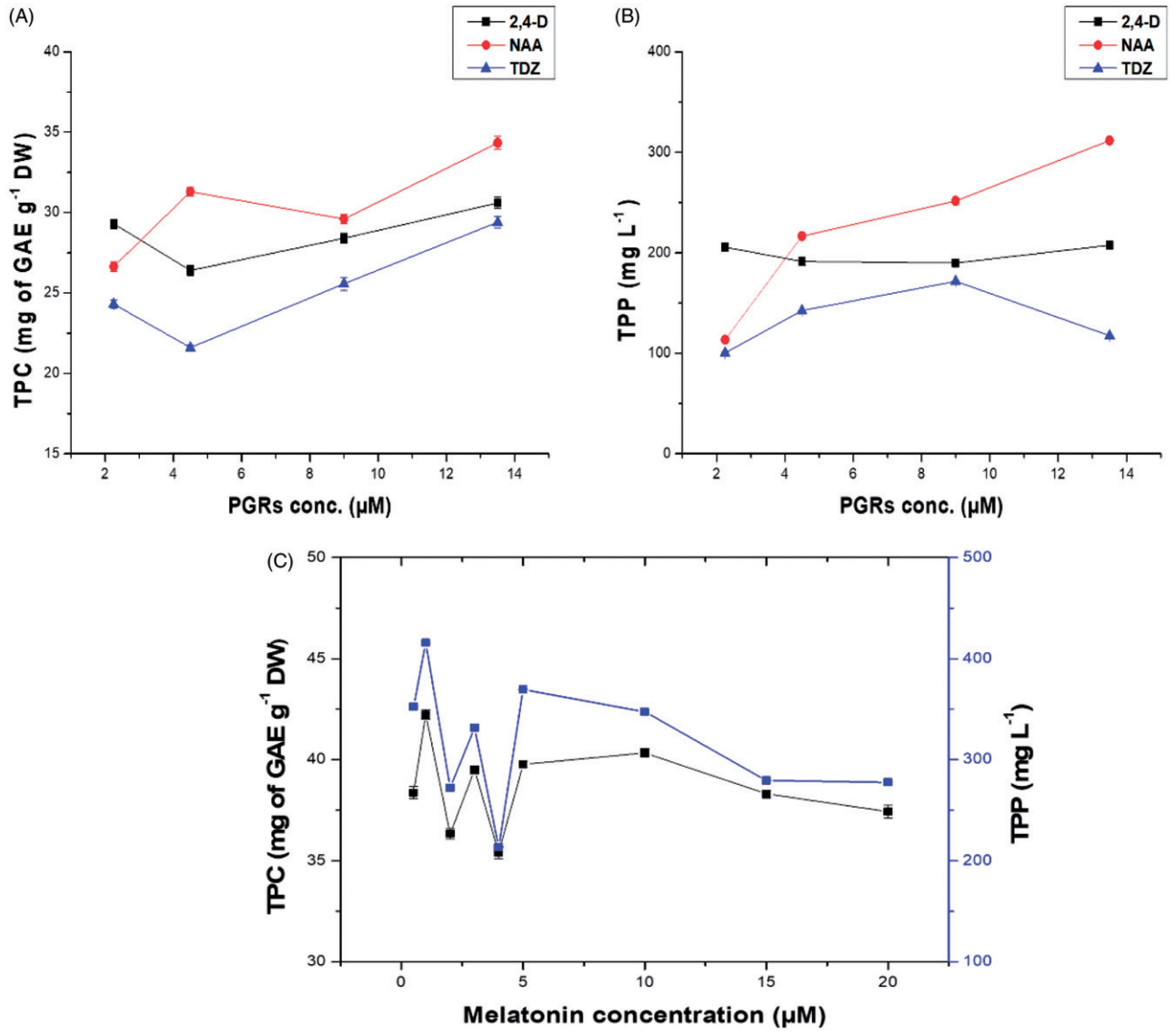

Figure 5. (A) Total phenolic content (TPC) of calli at different concentrations of NAA, 2,4-D and TDZ (B) Total phenolic production (TPP) of calli at different concentrations of NAA, 2,4-D and TDZ (C) TPC and TPP of calli at different concentrations of Melatonin +13.5 μM NAA.

actively [45]. Maximum TPC (35.2 mg of GAE g^{-1} DW) was recorded at the concentration of NAA (13.5 μM). Previously, TPC (30.8 mg of GAE g^{-1} DW) was reported by Akhtar et al. (2014) in *C. roseus* leaves [46]. Significant differences in TPC content (35.2 mg of GAE g^{-1} DW) was observed due to application of different PGRs in callus cultures of *C. roseus* (Figure 5(A)) [46–48]. Lowest TPC (15.8 mg of GAE g^{-1} DW) was recorded at 4.5 μM of TDZ (shown in the Figure 5(A)). TPC values were significantly increased with the application of melatonin. The highest value of TPC (42.23 mg of GAE g^{-1} DW) was recorded at 1.0 μM of melatonin and a notable increase in TPC content occurred when compared to the TPC value (35.2 mg of GAE g^{-1} DW) at 13.5 μM of NAA. Other concentrations of melatonin (0.5, 3, 5 and 10 μM) also showed considerable enhancement in TPC [38.5, 39.5, 39.40 and 40.33 mg of GAE g^{-1} DW; Figure 5(C)], respectively. Melatonin has been reported for enhanced phytochemical constituents and improved bio-reductive capacity [19]. Maximum TPP value (311.87 mg of GAE L^{-1}) at NAA 13.5 μM was recorded (Figure 5(B)). Around 415.41 mg of GAE L^{-1} was recorded at melatonin 1.0 μM (Figure 5(C)). TPP values (352.3, 331.4, 369.3 and 347.4 mg of GAE L^{-1}) recorded at 0.5, 3, 5 and 10 μM of melatonin, respectively, were remarkably different from TPP value of callus at the concentration of NAA (13.5 μM). Biomass accumulation and phenolic production are directly proportional and strongly dependent on the activation of key enzymes (tyrosine ammonia lyase) responsible for phytochemical production [41,49].

Estimation of total flavonoid content (TFC) and production (TFP)

Flavonoids are a class of phenolic compounds having antimicrobial, anti-oxidant, anti-inflammatory and allergenic activities [50]. Calli having different TFC strongly depends upon PGR type and concentration [38]. TFC value (29.36 mg of QUE g^{-1} DW) was recorded at the concentration of NAA 13.5 μM. Callus cultures of *C. roseus* showed a significant increase in TFC as compared to the reported value of TFC (11.4 mg of QUE/g SSDW) from the plant leaves [46]. Lowest TFC value

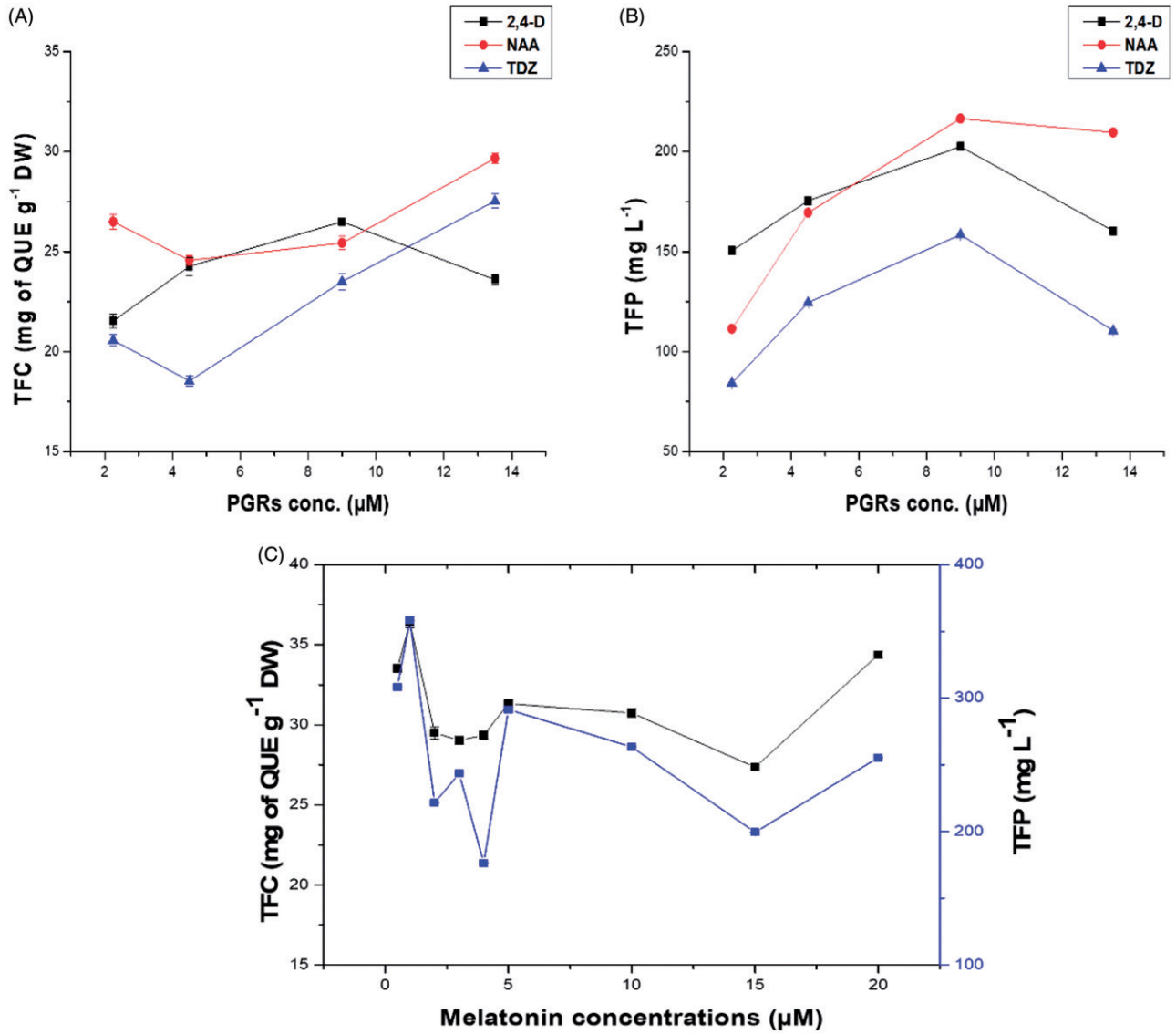

Figure 6. (A) Total flavonoid content (TFC) of calli at different concentrations of NAA, 2,4-D and TDZ (B) Total Flavonoid production (TFP) of calli at different concentrations of NAA, 2,4-D and TDZ (C) TFC and TFP of calli at different concentrations of Melatonin +13.5 μM NAA.

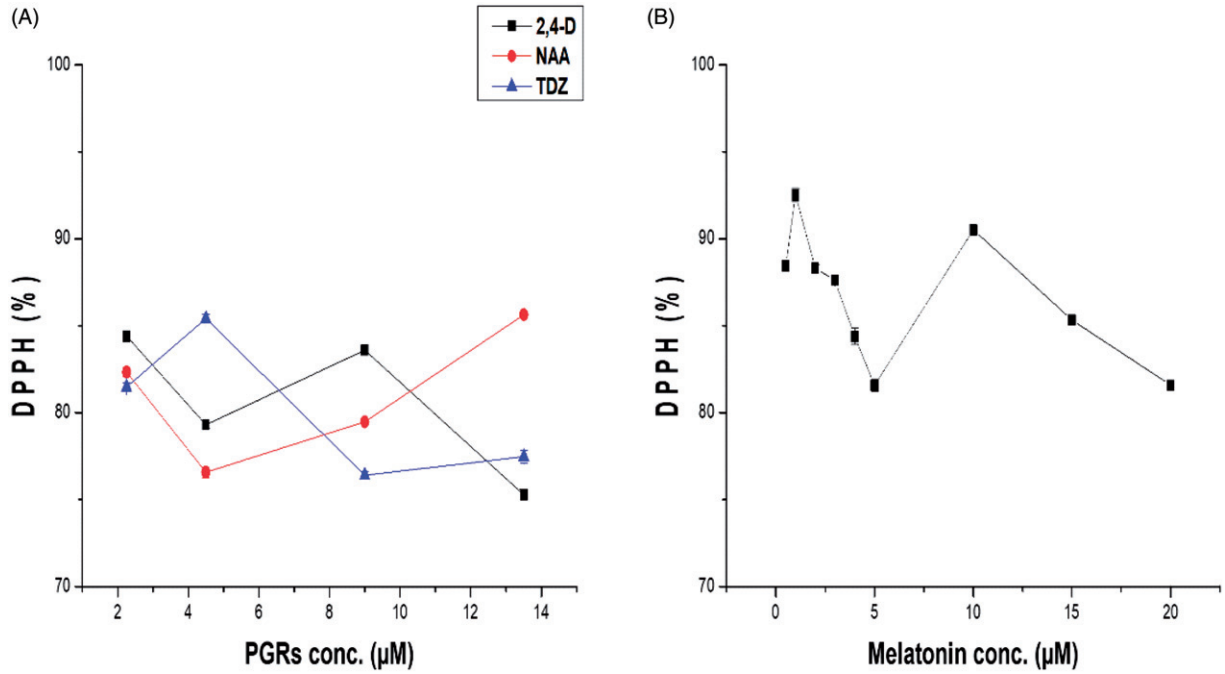

Figure 7. (A) DPPH: free radical scavenging activity (FRSA) of calli at different concentrations of NAA, 2,4-D, and TDZ (B) DPPH: free radical scavenging activity (FRSA) of calli at different concentrations of melatonin +13.5 μM of NAA.

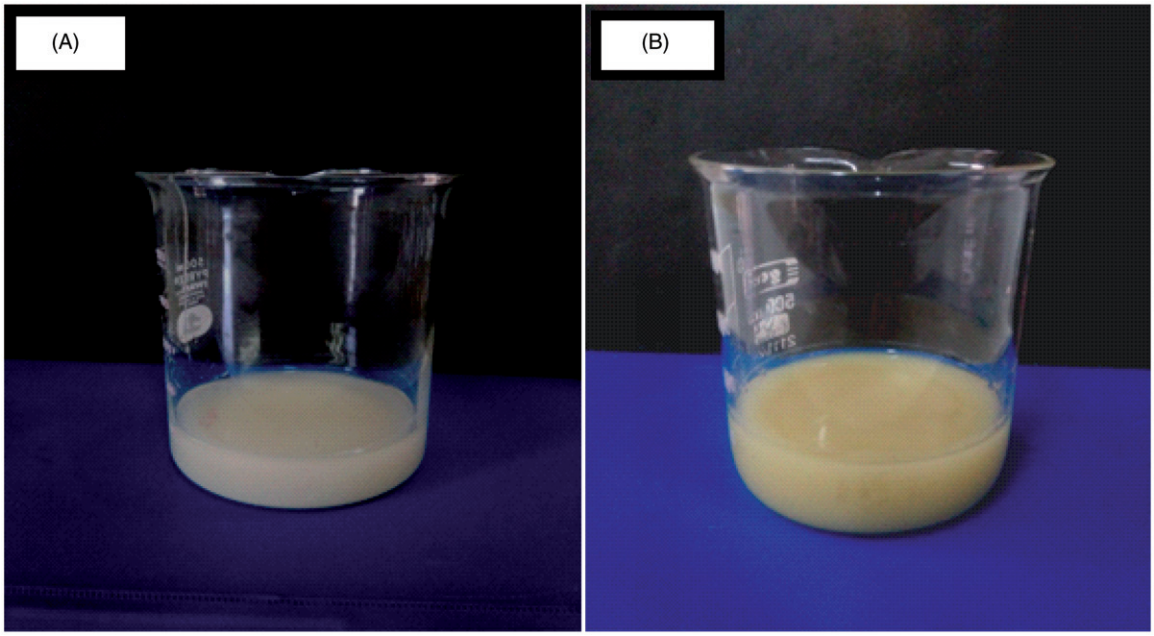

Figure 8. ZnONPs solution having (A) NAA CE (13.5 μM) (B) Mel + NAA CE (1.0 μM + 13.5 μM).

Table 3. Anti-bacterial assay of NAA CE and mel + NAA CE-mediated ZnO NPs.

	Zone of inhibition (mm) (20 μL well^{-1})						
Bacterial strains	Mel + NAA CE-mediated ZnO-NPs (1mg mL^{-1}), mean ± SD	NAA CE-mediated ZnO-NPs (1mg mL^{-1}), mean ± SD	WPE, (10 mg mL^{-1}), mean ± SD	Mel CE, (10 mg mL^{-1}), mean ± SD	NAA CE, (10 mg mL^{-1}), mean ± SD	Ampicillin, (10 μg mL^{-1}), mean ± SD	0.02 M ZADS mean ± SD
E. coli	10 ± 0.57	7 ± 1.25	–	8 ± 1.02	–	12 ± 1.52	7 ± 1.02
P. aeruginosa	13 ± 0.54	–	8 ± 0.57	–	–	10 ± 1.02	12 ± 1.52
B. subtilis	17 ± 0.76	13 ± 0.7		–	–	13 ± 1.15	7 ± 0.92

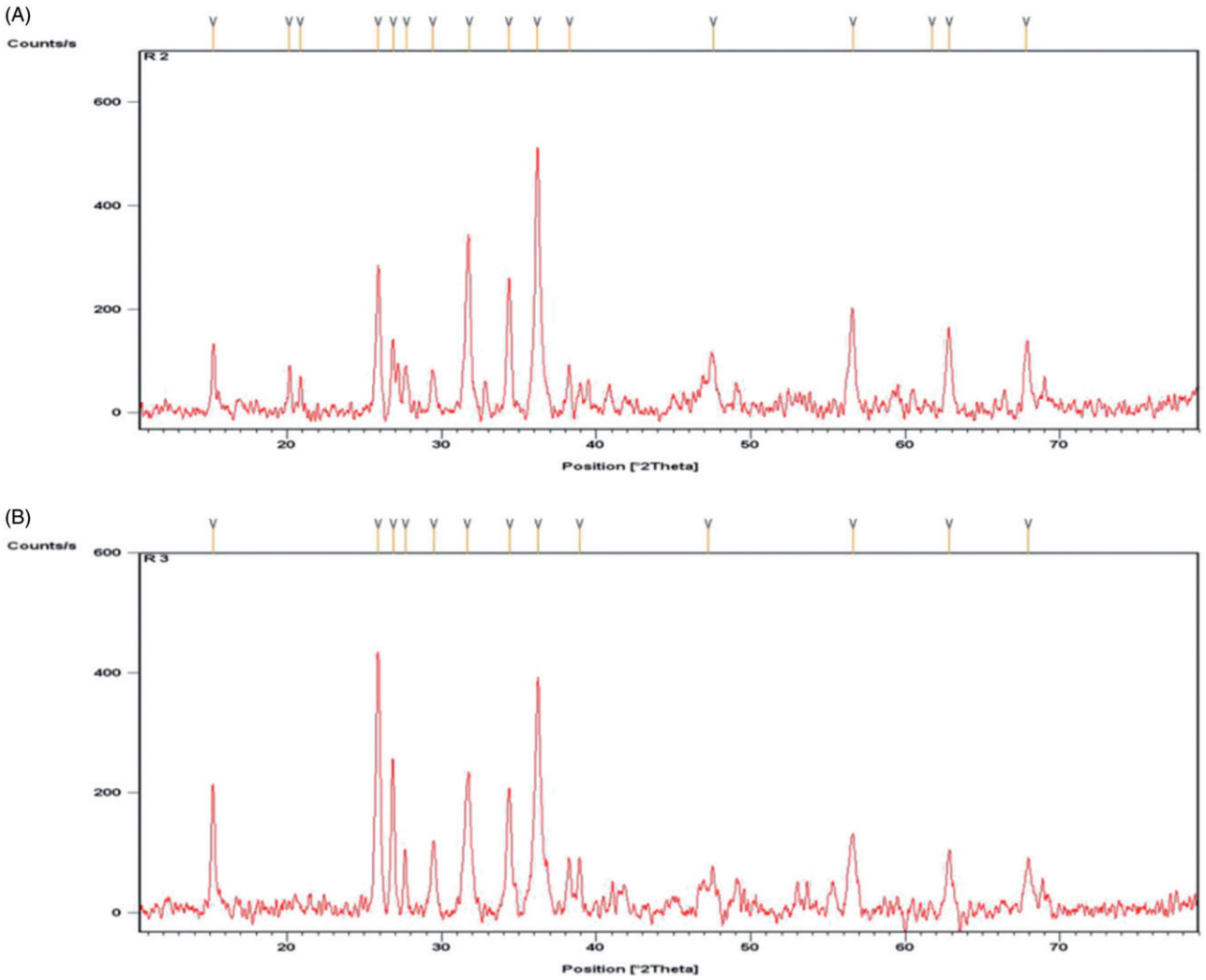

Figure 9. XRD pattern of (A) Control callus-mediated ZnONPs (B) Melatonin-induced callus-mediated ZnONPs.

(18.53 mg g^{-1}) was recorded at 4.5 μM of TDZ (Figure 6(A)). Melatonin (1.0 μM) showed maximum TFC (36.4 mg of QUE g^{-1} DW). 20, 10, 5 and 0.5 μM concentrations of melatonin also showed greater values of TFC (34.2 30.8 31.31 and 33.53 mg of QUE g^{-1} DW, respectively) as compared to NAA (13.5 μM).

Highest TFP value (209.54 mg of QUE L^{-1}) was recorded at 13.5 μM of NAA. 1.0 μM melatonin showed 358.2 mg of QUE L^{-1}. Other concentrations of melatonin (20, 10, 5 and 0.5 μM also showed a significant increase in TFP (255.02, 263.4, 291.3 and 308 mg of QUE L^{-1}, respectively).

DPPH (%): free-radical scavenging activity (FRSA)

FRSA represents the antioxidant status of plant and role of secondary metabolites as defensive agents against reactive oxygen species (ROS). Highest FRSA was 85.63% at the concentration of 13.5 μM of NAA and 4.5 μM of 2,4-D showed the lowest percentage (75.26%) of FRSA (Figure 7(A)). Callus induced in the presence of a 1.0 μM concentration of melatonin given the FRSA value of 92.51% as compared to callus with 13.5 μM of NAA (85.63%). Other concentrations of melatonin (15, 10, 3, 2 and 0.5 μM) showed significant increase in FRSA values (85.12%, 90.2%, 87.5%, 88.4% and 88.3, respectively) (Figure 7(B)). Calli produced in the presence of melatonin proved to be having highest reducing power (RP) because melatonin enhanced the phytochemical constituents (flavonoids and phenolics) in callus cultures of *C. roseus* by acting as good reductone (reductones are terminators of free radical chain reactions). Melatonin has been reported for higher antioxidant activity in different plants than other PGRs [51,52]. Bioactive compounds like flavonoids and phenolics acted as an electron donor and scavenge free radicals by converting them into more stable products and electron-donation capacity of the plant depends on the amount of bioactive compounds present in it [53]. Hence on the basis of the phytochemical analysis, callus produced at 13.5 μM of NAA was selected as control callus and will be compared with the callus produced at 1.0 μM of melatonin +13.5 μM of NAA (having highest phytochemical constituents) for further experimentation.

Synthesis of ZnONPs from NAA CE and mel + NAA CE

Phytochemicals (phenolics, tannins, proteins and flavonoids) carry out the reduction, capping and stabilization of NPs [54].

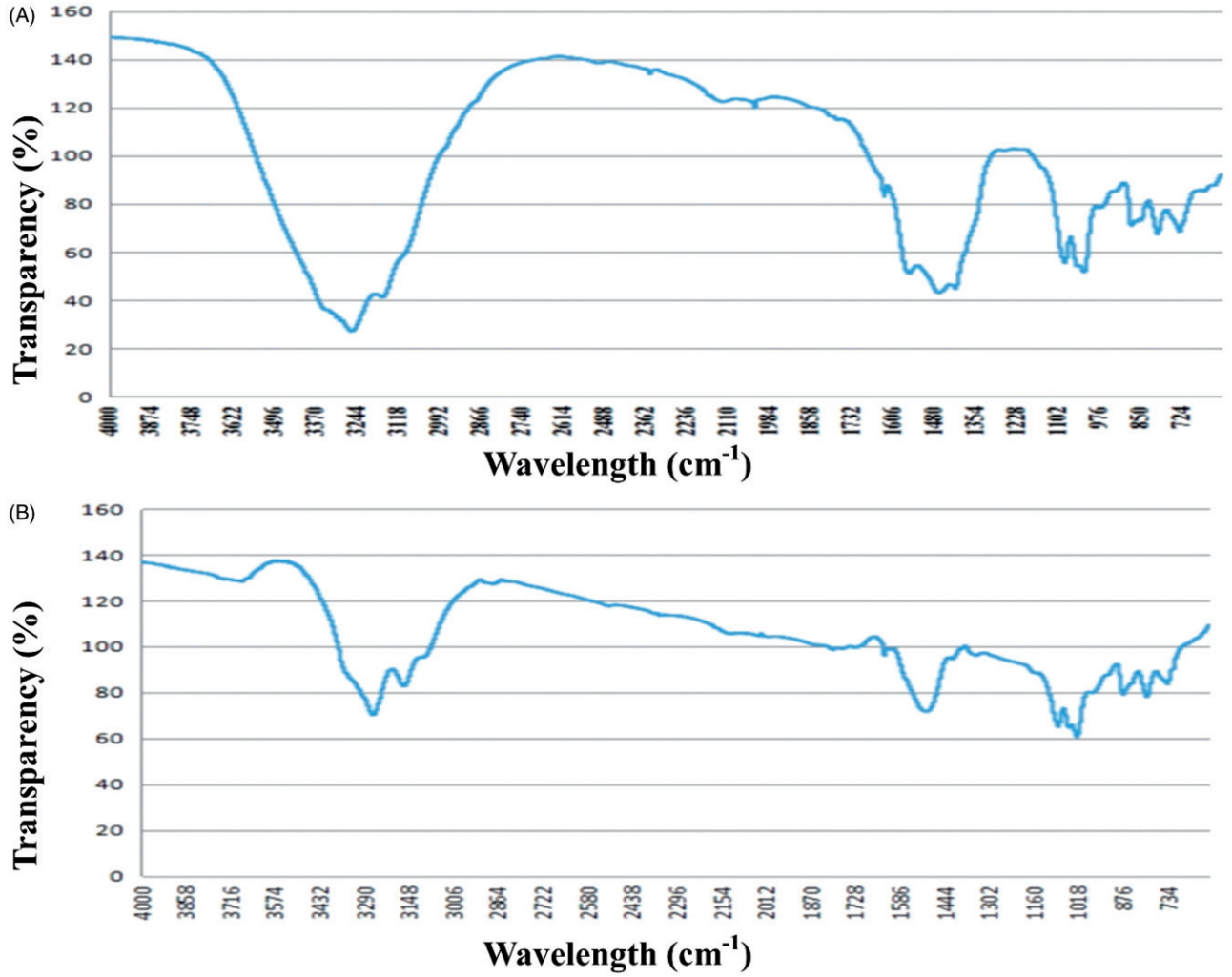

Figure 10. Fourier transform infrared (FTIR) spectra (A) NAA CE-mediated ZnONPs (B) Mel + NAA CE-mediated ZnONPs.

It was expected that these bioactive compounds will carry out the reduction and stabilization of ZnONPs, therefore NAA CE (13.5 μM) and Mel + NAA CE (1.0 μM + 13.5 μM) were separately mixed with 0.02 M ZADS (Figure 8). Pale-white precipitates (in the solution having NAA CE) and dark yellowish-pale precipitates (in the solution having Mel + NAA CE) appeared within 30 min after completing the reaction by constant stirring. The color change of solution from white to pale yellow indicate the synthesis of ZnONPs [7]. Darker color of the solution (having melatonin-induced callus extract) indicated the enhanced synthesis of ZnONPs [19]. Melatonin has been reported for enhanced AgNPs synthesis by improving bio-reducing potential [19]. Change in color was due to excitation of SPR (surface plasmon resonance) by absorption of visible light [55] (Table 3).

Characterization of ZnONPs

XRD analysis

Crystalline nature of ZnONPs was analyzed through XRD (Figure 9). In total, 13.5 μM NAA CE-mediated ZnONPs showed characteristic peaks at 2θ angles of 31.68°, 34.38°, 36.21°, 38.91°, 47.22°, 56.58°, S62.81° and 67.93° attributed to (100), (002), (101), (102), (110), (103) and (112). 1.0 μM Mel +13.5 μM NAA CE-mediated ZnONPs showed diffraction peaks at 2θ angles of 31.76°, 34.42°, 36.27°, 47.53°, 56.59°, 62.88° and 67.91° attributed to (100), (002), (101), (102), (110), (103) and (112). Results showed that NAA CE and Mel + NAA CE-mediated ZnONPs having hexagonal wurtzite structure (JCPDS file no: 36–1451). Average sizes of the ZnONPs were calculated by Debye-Scherrer Equation (1)

$$D = k\lambda / \beta \theta \cos. \quad (1)$$

NAA CE-mediated ZnO NPs having the size of 77.7 nm and Mel + NAA CE-mediated ZnONPs were smaller in size (64.5 nm). Sizes of ZnONPs were in agreement to the results obtained from SEM images. Smaller sized NPs played vital role as anti-bacterial agents by easily penetrating into the cell membranes [56].

Fourier transform infrared spectroscopy (FTIR) analysis

FTIR analysis was done to analyze different functional groups of bioactive reducing agents attached to the ZnONPs that were responsible for their reduction, capping and stabilization (Figure 10). A number of new absorption peaks at 3240 cm^{-1}, 3164 cm^{-1}, 3088 cm^{-1}, 2908 cm^{-1}, 2860 cm^{-1}, 1644 cm^{-1}, 1492 cm^{-1}, 1416 cm^{-1}, 1340 cm^{-1}, 1070 cm^{-1}, 1050 cm^{-1}, 1036 cm^{-1}, 1010 cm^{-1}, 960 cm^{-1}, 880 cm^{-1},

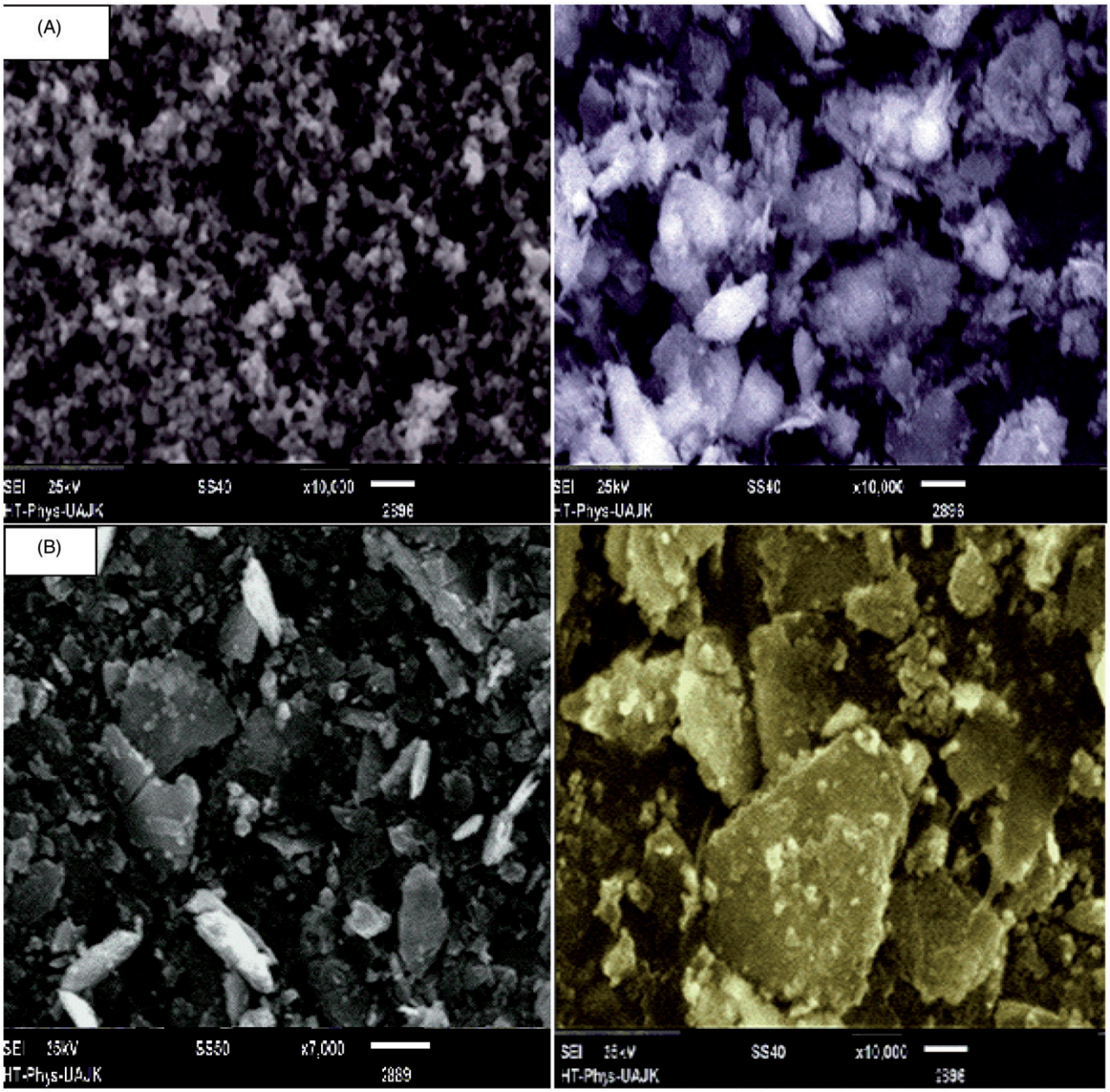

Figure 11. SEM images (A) control callus-mediated ZnONPs (B) Melatonin-induced callus-mediated ZnONPs.

808 cm^{-1} and 720 cm^{-1} appeared for NAA CE-mediated ZnONP while peaks at 3351 cm^{-1}, 3246 cm^{-1}, 2488 cm^{-1}, 2326 cm^{-1}, 2163 cm^{-1}, 2002 cm^{-1}, 1733 cm^{-1}, 1786 cm^{-1}, 1679 cm^{-1}, 1624 cm^{-1}, 1560 cm^{-1}, 1462 cm^{-1}, 1454 cm^{-1}, 1408 cm^{-1}, 1088 cm^{-1}, 1051 cm^{-1}, 1031 cm^{-1}, 964 cm^{-1}, 851 cm^{-1}, 784 cm^{-1}, 717 cm^{-1}, 651 cm^{-1}, 635 cm^{-1} and 620 cm^{-1} for Mel + NAA CE-mediated ZnONPs because of the reduction and capping of ZnO. These peaks corresponded to flavonoids, alcoholic and phenolic compounds. These respective peaks of O-H, C = O, C-H and C-C stretches are characteristics of flavonoids, alcoholic and phenolic compounds. Peaks in 2908 cm^{-1}–2860 cm^{-1} region correspond to the presence of O-H stretching in carboxylic groups. Peaks in 1600–1700 cm^{-1} region were due to the carbonyl (C = O) stretch. FTIR analysis showed that peaks in the region of 3300 cm^{-1}–2800 cm^{-1} were similar in NAA CE-mediated ZnONPs and Mel + NAA CE-mediated ZnONPs. Some additional peaks were also present in the Mel + NAA CE-mediated ZnONPs due to the presence of different phytochemicals. It was clearly shown that different phytochemicals carried out reduction, stabilization and capping of ZnONPs.

Scanning electron microscopy (SEM) analysis

SEM analysis was used to confirm the surface morphology of ZnONPs and images were taken at different magnifications shown in Figure 11. Spherical agglomerates of ZnO NPs synthesized from NAA CE were indicated by SEM images. Mel + NAA CE-mediated ZnONPs were triangular in shape and more scattered than NAA CE-mediated ZnONPs. SEM analysis also confirmed that smaller-sized NPs were capped by larger bioactive molecules thus avoiding agglomeration. Average sizes (77–79 nm) of ZnONPs synthesized from NAA CE and 58–64 nm of Mel + NAA CE-mediated ZnONPs were in

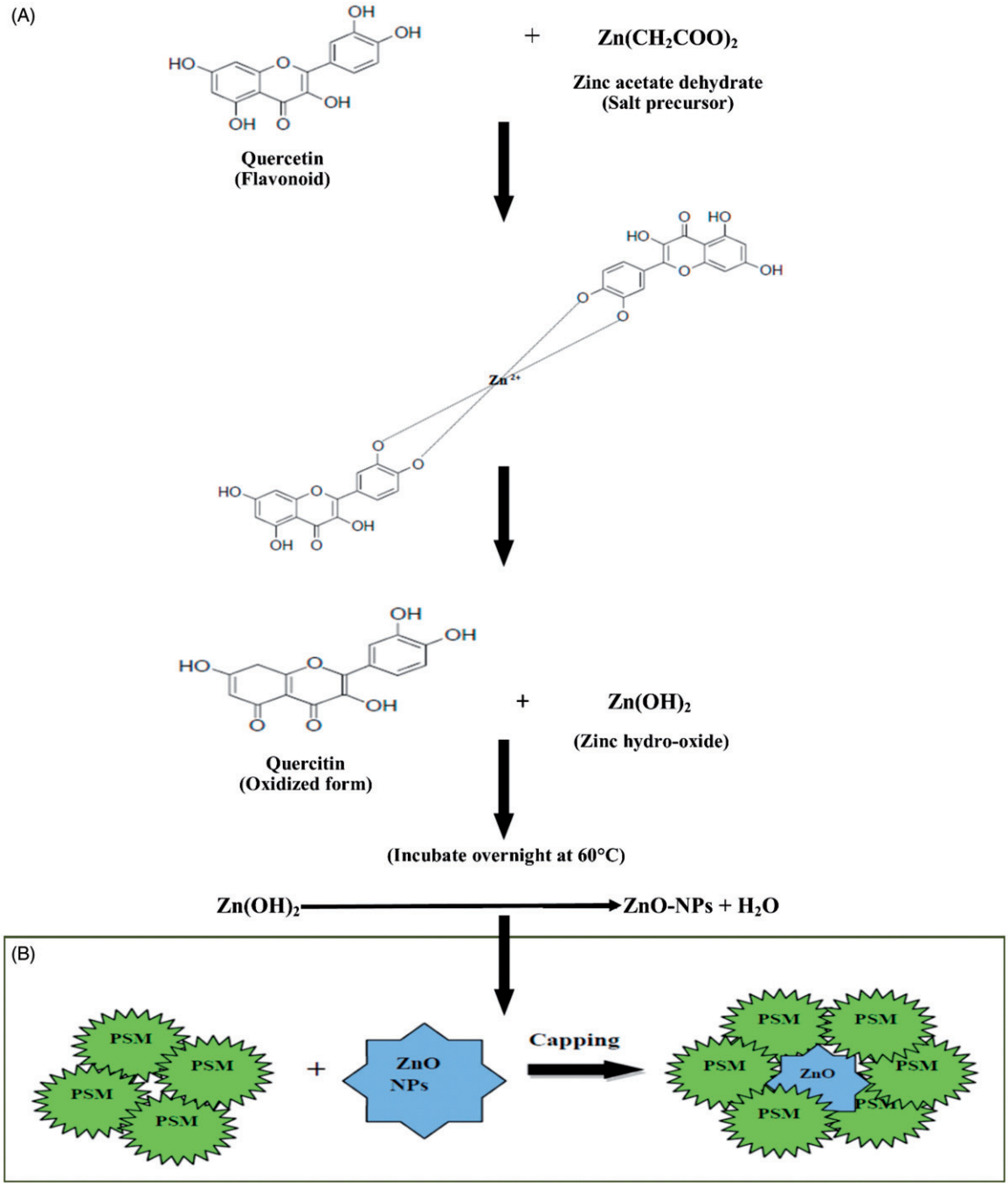

Figure 12. Proposed mechanism for the synthesis of ZnONPs (A) Flavonoid (quercetin) carried out the reduction of Zn^{2+} to Z^0 and quercetin (B) Capping and stabilization of ZnONPs by plant secondary metabolites (PSM).

great agreement with XRD analysis and indicated the presence of well-shaped ZnONPs.

Mechanism of ZnONPs

Mechanism involved in the synthesis of ZnONPs have not been fully explored, however, results from FTIR analysis indicates the presence of phenolics, flavonoids, alcoholic, carboxylic and carbonyl compounds in NAA CE and Mel + NAA CE-mediated ZnONPs, therefore proposed mechanism for ZnONPs synthesis was illustrated by using flavonoids (quercetin) present in *C. roseus*. OH, groups of quercetin, carried out the reduction of Z^{2+} ions to Z^0. Electron pair of OH group occupied empty orbital of Zn^{2+} ions by reducing it into the zero valent ions (Figure 12). Mechanisms for ZnONPs synthesis have been reported earlier and hypothesized with secondary metabolites [31,57].

Anti-bacterial activity

Anti-bacterial activities of characterized ZnONPs were evaluated against three bacterial strains, e.g. *E. coli, P. aeruginosa* and *B. subtilis*. Zones of inhibition were estimated in "mm". NAA CE-mediated ZnONPs produced the zone of inhibition

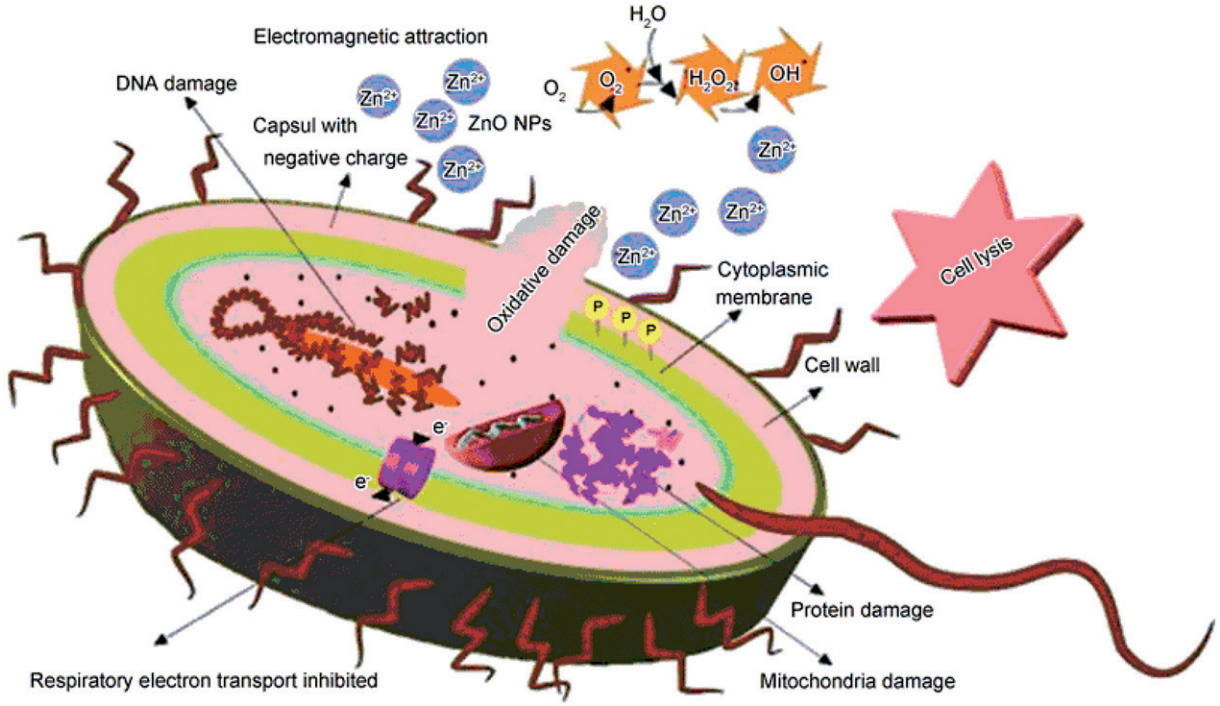

Figure 13. Anti-bacterial action of ZnONPs by interacting cell membrane and producing reactive oxygen species ultimately disrupts cell DNA and leads to the cell death.

7 ± 1.25 mm for *E. coli* and 13 ± 0.7 mm for *B. subtilis*. NAA CE-mediated ZnO-NPs did not show any zone of inhibition for *P. aeruginosa*. Mel + NAA CE-mediated ZnONPs were more active against bacterial strains and zones of inhibition were 10 ± 0.57 mm for *E. coli*, 13 ± 0.54 mm for *P. aeruginosa* and 17 ± 0.76 mm for *B. subtilis* (when compared with antibiotic ampicillin (12 ± 1.52 mm, 11 ± 1.02 mm and 13 ± 1.15 mm, respectively). ZnONPs have been reported for its anti-bacterial activities against *E. coli, P. aeruginosa* and *B. subtilis* [58]. WPE, melatonin callus extract (Mel CE) and NAA callus extract (NAA CE) showed a lower level of anti-bacterial activity as compared to the ZnONPs. Mel + NAA CE-mediated ZnONPs were more potent to anti-bacterial activities due to their smaller sizes. Smaller sized ZnONPs played vital role as anti-bacterial agents [56]. Smaller sized NPs can easily penetrate into the cells by causing the disruption of bacterial membrane [59]. ZnONPs activated by visible and UV-light and started producing H_2O_2 that penetrate into bacterial membrane and cause disruption [60].

Mechanism of anti-bacterial activities for ZnONPs

The mechanism behind anti-bacterial activities of ZnONPs have not been fully illustrated in previous reports, therefore, a hypothesized mechanism for the anti-bacterial action of ZnONPs has been proposed in terms of bacterial cell-membrane permeability. Activities of ZnONPs mainly depends on their physical properties (shape and size) and physio-chemical properties [61,62]. Smaller-sized ZnONPs easily penetrate into the bacterial cell via cell membrane and starts interacting with cell organelles (Figure 13). ROS were generated by disrupting DNA replication. Along with ROS (O_2^-, OH^- and H_2O_2), Zn^{2+} ions also released and damage the cell membrane. Cytoplasmic-leakage ultimately leads to the cell death. ROS based mechanisms for bacterial cell death has been reported previously for ZnONPs [63–65].

Conclusion

In this report, the potential of melatonin as PGR and its ability to synthesize ZnO-NPs was studied in the callus cultures of *C. roseus* var. *alba*. The production of phytochemicals in callus cultures of *C. roseus* was improved by applying melatonin exogenously. These phytochemicals carried out the reduction, stabilization and capping of ZnONPs. NAA CE and Mel + NAA CE-mediated ZnONPs were compared. Mel + NAA CE-mediated ZnONPs were rapidly synthesized and these NPs were more scattered, triangular and possess the higher anti-bacterial activity than that of NAA CE-mediated ZnO-NPs. This study promises to open new ways of using melatonin for increasing bioactive reducing agents in callus cultures and boosting the NPs synthesis and their potential use in biomedical applications.

Disclosure statement

No potential conflict of interest was reported by the author(s).

References

[1] Hristozov D, Ertel J. Nanotechnology and sustainability: benefits and risks of nanotechnology for environmental sustainability. Forum Der Forschung. 2009;22:161–168.

[2] Hussain I, Singh N, Singh A, et al. Green synthesis of nanoparticles and its potential application. Biotechnol Lett. 2016;38:545–560.
[3] Khan ST, Musarrat J, Al-Khedhairy AA. Countering drug resistance, infectious diseases, and sepsis using metal and metal oxides nanoparticles: current status. Colloids Surf B Biointerfaces. 2016;146:70–83.
[4] Iravani S. Green synthesis of metal nanoparticles using plants. Green Chem. 2011;13:2638–2650.
[5] Madhumitha G, Elango G, Roopan SM. Biotechnological aspects of ZnO nanoparticles: overview on synthesis and its applications. Appl Microbiol Biotechnol. 2016;100:571–581.
[6] Gunalan S, Sivaraj R, Rajendran V. Green synthesized ZnO nanoparticles against bacterial and fungal pathogens. Pro Nat Sci Mater: Mater Int. 2012;22:693–700.
[7] Dobrucka R, Długaszewska J. Biosynthesis and antibacterial activity of ZnO nanoparticles using *Trifolium pratense* flower extract. Saudi J Biol Sci. 2016;23:517–523.
[8] Atarod M, Nasrollahzadeh M, Sajadi SM. Green synthesis of Pd/RGO/Fe3O4 nanocomposite using *Withania coagulans* leaf extract and its application as magnetically separable and reusable catalyst for the reduction of 4-nitrophenol. J Colloid Interface Sci. 2016;462:272–279.
[9] Ahmed S, Ahmad M, Swami BL, et al. A review on plants extract mediated synthesis of silver nanoparticles for antimicrobial applications: a green expertise. J Adv Res. 2016;7:17–28.
[10] Alagumuthu G, Kirubha R. Green synthesis of silver nanoparticles using *Cissus quadrangularis* plant extract and their antibacterial activity. Ojsta. 2012;2:30–33.
[11] Singh P, Kim Y, Zhang JD, Yang D-C. Biological Synthesis of Nanoparticles from Plants and Microorganisms. Trends in biotechnology. Trends Biotechnol. 2016;34:588–599.
[12] Sain M, Sharma V. *Catharanthus roseus* (An anti-cancerous drug yielding plant) - A Review of Potential Therapeutic Properties. Int J Pure App Biosci. 2013;1:139–142.
[13] Verma AK, Singh R, Singh S. Improved alkaloid content in callus culture of *Catharanthus roseus*. Bot Serbica. 2012;36:123–130.
[14] Almagro L, Fernández-Pérez F, Pedreño MA. Indole Alkaloids from *Catharanthus roseus*: bioproduction and their effect on human health. Molecules. 2015;20:2973–3000.
[15] Gajalakshmi S, Vijayalakshmi S, Devi RV. Pharmacological activities of *Catharanthus roseus*: a perspective review. Int J Pharma Bio Sci. 2013;4:431–439.
[16] MoudiGo MR, Yien CYS, Nazre M. Vinca alkaloids. Int J Prevent Med. 2013;4:1231–1235.
[17] Stavrinides A, Tatsis EC, Foureau E, et al. Unlocking the diversity of alkaloids in *Catharanthus roseus*: nuclear localization suggests metabolic channeling in secondary metabolism. Chem Biol. 2015;22:336–341.
[18] Schutz FA, Bellmunt J, Rosenberg JE, et al. Vinflunine: drug safety evaluation of this novel synthetic vinca alkaloid. Expert Opin Drug Saf. 2011;10:645–653.
[19] Sheshadri S, Sriram S, Balamurugan P, et al. Melatonin improves bioreductant capacity and silver nanoparticles synthesis using *Catharanthus roseus* leaves. Phenolic compounds in *Catharanthus roseus*. Verpoorte RSC Adv. 2015;5:47548–47554.
[20] Mustafa NR, Verpoorte R. Phenolic compounds in *Catharanthus roseus*. Verpoorte. Phytochem Rev. 2007;6:243–258.
[21] Gaspar T, Kevers C, Penel C, et al. Plant hormones and plant growth regulators in plant tissue culture. In Vitro Cell Dev Biol Plant. 1996;32:272–289.
[22] Karthikeyan B, Jaleel CA, Gopi R, et al. Alterations in seedling vigour and antioxidant enzyme activities in *Catharanthus roseus* under seed priming with native diazotrophs. J Zhejiang Univ – Sci B. 2007;8:453–457.
[23] Patel H, Krishnamurthy R. Elicitors in plant tissue culture. J Pharmacognosy Phytochemist. 2013;2:60–65.
[24] Lerner AB, Case JD, Takahashi Y, et al. Isolation of melatonin, the pineal gland factor that lightens melanocytes. J Am Chem Soc. 1958; 80:2587–2587.
[25] Arnao MB. Phytomelatonin: discovery, content, and role in plants. Adv Bot. 2014;2014:815769.
[26] Arnao MB, Hernández-Ruiz J. The Physiological Function of Melatonin in Plants. Plant Signal Behav. 2006;1:89–95.
[27] Pelagio-Flores R, Ortíz-Castro R, Méndez-Bravo A, et al. Serotonin, a tryptophan-derived signal conserved in plants and animals, regulates root system architecture probably acting as a natural auxin inhibitor in *Arabidopsis thaliana*. Plant Cell Physiol. 2011;52:490–508.
[28] Arnao M, Hernández-Ruiz J. Protective effect of melatonin against chlorophyll degradation during the senescence of barley leaves. J Pineal Res. 2009;46:58–63.
[29] LiHe H, Yang J, Li X, et al. Glutathione-dependent induction of local and systemic defense against oxidative stress by exogenous melatonin in cucumber (*Cucumis sativus* L.). J Pineal Res. 2016;60:206–216.
[30] Murch SJ, Saxena PK. Melatonin: a potential regulator of plant growth and development? In Vitro Cell Dev Biol Plant. 2002;38:531–536.
[31] Abbasi BH, Khan MA, Mahmood T, et al. Shoot regeneration and free-radical scavenging activity in *Silybum marianum L*. Plant Cell Tiss Organ Cult. 2010;101:371–376.
[32] Singleton V, Rossi JA. Colorimetry of Total Phenolics with Phosphomolybdic-Phosphotungstic Acid Reagents. Am J Enol Viticulture. 1965;16:144–158.
[33] Ul-Haq I, Ullah N, Bibi G, et al. Antioxidant and Cytotoxic Activities and Phytochemical Analysis of *Euphorbia wallichii* Root Extract and its Fractions. Iranian J Pharmaceut Res: IJPR. 2012;11:241.
[34] Rattanachitthawat S, Suwannalert P, Riengrojpitak S, et al. Phenolic content and antioxidant activities in red unpolished Thai rice prevents oxidative stress in rats. J Med Plants Res. 2010;4:796–801.
[35] Azam A, Ahmed A, Oves SM, et al. Antimicrobial activity of metal oxide nanoparticles against Gram-positive and Gram-negative bacteria: a comparative study. Int J Nanomed. 2012;7:6003.
[36] Upadhyaya G, Sen M, Roy A. In vitro callus induction and plant regeneration of rice (*Oryza sativa* L.) var. 'Sita', 'Rupali' and 'Swarna Masuri'. Asian J Plant Sci Res. 2015;5:24–27.
[37] Sheeba E, Palanivel S, Parvathi S. Effect of plant growth regulators on callus induction in *Physalis minima* Linn. Ijirset. 2013;2:4847–4851.
[38] Arif M, Rauf S, Din AU, et al. High Frequency Plant Regeneration from Leaf Derived Callus of *Dianthus caryophyllus* L. Ajps. 2014;5:2454.
[39] Hussain Z, Khan MH, Bano R, et al. Protocol optimization for efficient callus induction and regeneration in three pakistani rice cultivars. Pak J Bot. 2010;42:879–887.
[40] Skoog F, Miller C. Chemical regulation of growth and organ formation in plant tissues cultured in vitro. Symp Soc Exp Biol. 1957;11:118–131.
[41] Ali M, Abbasi BH. Thidiazuron-induced changes in biomass parameters, total phenolic content, and antioxidant activity in callus cultures of *Artemisia absinthium* L. Appl Biochem Biotechnol. 2014;172:2363–2376.
[42] Gill R, Ozias-Akins P. Thidiazuron-induced highly morphogenic callus and high frequency regeneration of fertile peanut (*Arachis hypogaea* L.) plants. In Vitro Cell Dev Biol Plant. 1999;35:445–450.
[43] Einset JW. Two Effects of Cytokinin on the Auxin Requirement of Tobacco Callus Cultures. Plant Physiol. 1977;59:45–47.
[44] Murch SJ, Campbell SS, Saxena PK. The role of serotonin and melatonin in plant morphogenesis: regulation of auxin-induced root organogenesis in in vitro-cultured explants of St. John's wort (*Hypericum perforatum* L.). In Vitro Cell Dev Biol Plant. 2001;37:786–793.
[45] Ainsworth EA, Gillespie KM. Estimation of total phenolic content and other oxidation substrates in plant tissues using Folin-Ciocalteu reagent. Nat Protoc. 2007;2:875.
[46] Akhtar N, Ihsan-ul-haq, Mirza B. Phytochemical analysis and comprehensive evaluation of antimicrobial and antioxidant properties

of 61 medicinal plant species. Arab J Chem. 2015. DOI:10.1016/j.arabjc.2015.01.013.
[47] Pan Q, Chen Y, Wang Q, et al. Effect of Plant Growth Regulators on the Biosynthesis of Vinblastine, Vindoline and Catharanthine in *Catharanthus roseus*. Plant Growth Regulat. 2010;60:133–141.
[48] Idrees M, Naeem M, Aftab T, et al. Salicylic acid mitigates salinity stress by improving antioxidant defence system and enhances vincristine and vinblastine alkaloids production in periwinkle [*Catharanthus roseus*]. Acta Physiologiae Plantarum. 2011;33:987–999.
[49] Ali M, Abbasi BH. Production of commercially important secondary metabolites and antioxidant activity in cell suspension cultures of *Artemisia absinthium L*. Ind Crops Prod. 2013;49:400–406.
[50] Pietta P-G. Flavonoids as antioxidants. J Nat Prod. 2000;63:1035–1042.
[51] Van Tassel DL, O'neill SD. Putative regulatory molecules in plants: evaluating melatonin. J Pineal Res. 2001;31:1–7.
[52] Posmyk MM, Janas KM. Melatonin in plants. Acta Physiol Plant. 2009;31:1.
[53] Gordon M. The mechanism of antioxidant action in vitro. In: Hudson BJF, editor. Food antioxidants. London: Elsevier Applied Science; 1990. p. 1–18.
[54] Kołodziejczak-Radzimska A, Jesionowski T. Zinc Oxide—From Synthesis to Application: a Review. Materials (Basel). 2014;7:2833–2881.
[55] Serrano A, Rodríguez de la Fuente O, Collado V, et al. García. Simultaneous surface plasmon resonance and x-ray absorption spectroscopy. Rev Sci Instrum. 2012;83:083101.
[56] Arokiyaraj S, Arasu MV, Vincent S, et al. Rapid green synthesis of silver nanoparticles from *Chrysanthemum indicum L* and its antibacterial and cytotoxic effects: an in vitro study. Int J Nanomed. 2014;9:379.
[57] Bala N, Saha S, Chakraborty M, et al. Green synthesis of zinc oxide nanoparticles using *Hibiscus subdariffa* leaf extract: effect of temperature on synthesis, anti-bacterial activity and anti-diabetic activity. RSC Adv. 2015;5:4993–5003.
[58] Govindasamy C, Srinivasan R. In vitro antibacterial activity and phytochemical analysis of *Catharanthus roseus* (Linn.) G. Don. Asian Pacific J Trop Biomed. 2012;2:S155–S158.
[59] Morones JR, Elechiguerra JL, Camacho A, et al. The bactericidal effect of silver nanoparticles. Nanotechnology. 2005;16:2346.
[60] Das B, Dash S, Mandal K, et al. Green synthesized silver nanoparticles destroy multidrug resistant bacteria via reactive oxygen species mediated membrane damage. Arab J Chem. 2015;10:862–876.
[61] Jones N, Ray B, Ranjit KT, et al. Antibacterial activity of ZnO nanoparticle suspensions on a broad spectrum of microorganisms. FEMS Microbiol Lett. 2008;279:71–76.
[62] Brayner R, Ferrari-Iliou R, Brivois N, et al. Toxicological Impact Studies Based on *Escherichia coli* Bacteria in Ultrafine ZnO Nanoparticles Colloidal Medium Nano Lett. 2006;6:866–870.
[63] Jalal R, Goharshadi EK, Abareshi M, et al. ZnO nanofluids: green synthesis, characterization, and antibacterial activity. Mater Chem Phys. 2010;121:198–201.
[64] Padmavathy N, Vijayaraghavan R. Enhanced Bioactivity of ZnO Nanoparticles an Antimicrobial Study. Sci Technol Adv Mater. 2008;9:035004.
[65] Yamamoto O. Influence of particle size on the antibacterial activity of zinc oxide. Int J Inorg Mater. 2001;3:643–646.